A new method to measure local oxygen consumption in human skeletal muscle during dynamic exercise using near-infrared spectroscopy

2010 Physiol. Meas. 31 1257

(http://iopscience.iop.org/0967-3334/31/9/014)

IOP PUBLISHING PHYSIOLOGICAL MEASUREMENT

Physiol. Meas. **31** (2010) 1257–1269 doi:10.1088/0967-3334/31/9/014

A new method to measure local oxygen consumption in human skeletal muscle during dynamic exercise using near-infrared spectroscopy

Tiziano Binzoni[1,2], Chris E Cooper[3], Anna L Wittekind[3], Ralph Beneke[3], Clare E Elwell[4], Dimitri Van De Ville[2,5] and Terence S Leung[4]

[1] Département des Neurosciences Fondamentales, University of Geneva, Geneva, Switzerland
[2] Département de l'Imagerie et des Sciences de l'Information Médicale, University Hospital, Geneva, Switzerland
[3] Department of Biological Sciences, University of Essex, Colchester Essex, UK
[4] Department of Medical Physics and Bioengineering, University College London, London, UK
[5] Institute of Bioengineering, Ecole Polytechnique Fédérale de Lausanne (EPFL), Lausanne, Switzerland

E-mail: tiziano.binzoni@unige.ch

Received 9 February 2010, accepted for publication 9 July 2010
Published 11 August 2010
Online at stacks.iop.org/PM/31/1257

Abstract

Near infrared spectroscopy (NIRS) can readily report on changes in blood volume and oxygenation. However, it has proved more problematic to measure real-time changes in blood flow and oxygen consumption. Here we report the development of a novel method using NIRS to measure local oxygen consumption in human muscle. The method utilizes the blood volume changes induced by the muscle pump during rhythmically contracting exercising skeletal muscle. We found that the saturation of the blood during the contraction phase was lower than that during the relaxation phase. The calculated oxygen drop was then divided by the contraction time to generate a value for the muscle oxygen consumption in the optical region of interest. As a test we measured the muscle oxygen consumption in the human *vastus lateralis* during exercise on a cycle ergometer by 11 trained male athletes (32 ± 11 years old) at 40% and 110% peak aerobic power. We saw an increase from 13.78 μmol 100 g^{-1} min^{-1} to 19.72 μmol 100 g^{-1} min^{-1} with the increase in power. The measurements are theoretically exempt from usual NIRS confounders such as myoglobin and adipose tissue and could provide a useful tool for studying human physiology.

Keywords: human, oxygen consumption, NIRS, blood oxygen saturation, exercise

(Some figures in this article are in colour only in the electronic version)

1. Introduction

The present contribution aims to non-invasively assess local arterial blood oxygen saturation and oxygen consumption ($\dot{O}_{2m}$) in human skeletal muscle during dynamic exercise. To obtain $\dot{O}_{2m}$, the initial step comprises the simultaneous measurement of the instantaneous haemoglobin oxygen saturation (SO_2) of the *net* blood flow entering/leaving the observed region of interest (ROI) and the instantaneous tissue haemoglobin concentration ([Hb_{tot}]; where [ ] denotes concentration) changes. Then, $\dot{O}_{2m}$ is obtained by combining in a suitable manner SO_2, [Hb_{tot}] and their relationship that ensues from the classical Fick approach (Berne and Levy 1998).

SO_2 represents in itself a fundamental parameter in human skeletal muscle physiology, because it is intimately linked to at least two important mechanisms: (1) blood flow regulation and (2) oxidative energy metabolism. The SO_2 level is known to influence ATP release from the erythrocytes and the resulting intravascular ATP concentration modulates at its turn the vascular tone through the interaction with specific receptors present on the vascular wall (Ellsworth *et al* 2009). Moreover, well-saturated haemoglobin acts also as NO scavenger, and thus SO_2 decrease may have an indirect influence on tissue blood perfusion (Boushel 2003). In this manner, SO_2 appears to be one of the key elements controlling the biochemical cascade that modulates the blood supply to the tissue. On the other hand, the knowledge of blood flow and SO_2 values on the arterial and venous sides allows human physiologists to assess muscle $\dot{O}_{2m}$ by means of the well-known Fick principle (Berne and Levy 1998). These observations highlight the importance of determining SO_2 values at different positions along the blood vessels. Without SO_2 spatial information, it is usually considered impossible to estimate $\dot{O}_{2m}$ by means of the Fick principle or to realize reliable studies on the relationship between SO_2 and blood flow regulation.

In humans, the ability to assess SO_2 non-invasively represents a difficult task and the existing methods are mainly based, directly or indirectly, on near-infrared spectroscopy (NIRS) techniques. We can roughly divide these methods in two categories: (1) 'pure' near-infrared-based techniques allowing us to obtain a global mean SO_2-value of the venous/arterial sides of the vascular tree (see, for a review, McCully and Hamaoka (2000), Rolfe (2000), Boushel *et al* (2001), Quaresima *et al* (2003), Bhambhani (2004), Ferrari *et al* (2004), Hamaoka *et al* (2007), Wolf *et al* (2007)); the techniques consist of a combination of near-infrared light sources, detectors and specialized algorithms; and (2) vascular imaging techniques such as photoacoustic imaging allowing us to obtain 3D images of the vascular tree, and the SO_2 values of the imaged vessels can be colour-coded (see, for a review, Wang (2008), (2009), Haisch (2009)); the technique use a combination of infrared laser light sources, ultrasound detectors and related mathematical algorithms. Photoacoustic 3D-imaging is theoretically the solution of choice because it allows us to obtain SO_2 values at each point along the observed vessels (Zhang *et al* 2009). Unfortunately, this technique cannot be applied on exercising human skeletal muscle. In fact, the location depth of the observed vascular tree (e.g. >1 cm under the skin layer) or the muscle movements limit the applicability of this method. On the other hand, 'pure' near-infrared-based techniques seriously restrict SO_2 spatial localization, i.e. they allow us to obtain only one global SO_2 value of the observed muscle ROI. This limitation prevents us from exploiting SO_2 data to derive $\dot{O}_{2m}$ and it appears, at first sight, an insurmountable problem for the present work.

The aim of this paper is to show that while the 'pure' near-infrared-based measurement technique comes with poor spatial resolution, it does allow us to assess local oxygen saturation of the blood entering the muscle ROI and $\dot{O}_{2m}$ during dynamic exercise. In our previous work, we reported a new way to calculate the local tissue oxygen saturation based on the

repeated cycles of muscle contraction and relaxation occurring when skeletal muscle is made to contract rhythmically (Leung *et al* 2010). Oxygen extraction occurs during this 'muscle pump' (Lutjemeier *et al* 2008). Therefore it is possible to use this 'cyclic' signal embedded in the NIR signal to derive instantaneous oxygen saturation and $\dot{O}_{2m}$.

The proposed approach is non-invasive and does not need any physiological manipulation such as venous or arterial occlusions (Cheatle *et al* 1991, De Blasi *et al* 1993). To the best of our knowledge, this is the first non-invasive technique allowing us to estimate local instantaneous oxygen saturation and $\dot{O}_{2m}$ during dynamic exercise. We hope that this preliminary contribution will provide the scientific community with a supplementary non-invasive tool allowing the investigation of muscle physiology in humans.

2. Material and methods

2.1. Subjects

The study was conducted on 11 male trained cyclists/triathletes aged 32 ± 11 year, body mass 77 ± 8 kg, stature 177 ± 6 cm. The study was approved by the University of Essex Ethics Committee in accordance with standards set down by the Declaration of Helsinki. The test procedures and possible risks were explained to each subject prior to obtaining written informed consent.

2.2. Experimental protocol

Participants visited the laboratory on two occasions separated by at least 48 h.

During the first experimental session the subjects undertook an incremental load test on an electrodynamically braked cycle ergometer (Lode Excalibur Sport, Groningen, The Netherlands) to determine their peak aerobic power (PAP) and peak oxygen consumption ($\dot{V}O_{2peak}$). The test started with a work load of 1.0 W kg^{-1} and was increased by 0.5 W kg^{-1} every 2 min until volitional exhaustion or the subject could no longer maintain the specified pedal rate of 80 rpm. PAP was defined as the final power achieved if the test was terminated at the end of a 2 min stage. If the test was terminated before the last stage had been completed, PAP was calculated as the power of the previous stage plus the power increment times the duration of exercise at the final stage divided by 120 s. The $\dot{V}O_{2\,peak}$ was calculated as the highest $\dot{V}O_2$ for any 30 s period. The result of this test was used to determine the intensities of the second session. The mean values for $\dot{V}O_{2\,peak}$ and PAP were 60 ± 5 ml kg^{-1} min^{-1} and 4.78 ± 0.56 W kg^{-1}, respectively.

During the second session, muscle (*vastus lateralis*) instantaneous oxy- and deoxy-haemoglobin concentration ([HbO_2] and [Hb], respectively) changes were assessed by NIRS (see below), for two different exercise intensities on a mechanically braked cycle ergometer (Monark 824 Ergomedic, Varberg, Sweden). This exercise consisted of a 5 min work load at 40% PAP (60 rpm = 1 pedal cycle s^{-1}) immediately followed by 1 min at 110% (80 rpm = $1.\bar{3}$ pedal cycles s^{-1}).

Participants could use their own pedals and cycle shoes on all tests.

2.3. Arterial oxygen saturation

The arterial saturation was measured by pulse oximetry (Ohmeda Biox III, BOC Health Care, Boulder, CO, USA) at the earlobe. The mean SO_2 for the last 20 s at 40% PAP was 95.5 ± 1.5%. The corresponding value for the last 10 s at 110% PAP was 92.2 ± 3.4%.

2.4. Measurement of $\dot{V}O_2$

Pulmonary gas exchange was measured breath-by-breath throughout all tests with a gas analyser (OxyconPro, Viasys Healthcare, Warwick, UK). Participants wore a small or medium adult face mask of low dead space with all gas measurements corrected for dead space. The face mask was connected to a low-resistance triple-V volume transducer which was calibrated according to manufacturer instructions before each test. The gas analysers were calibrated at the start of each testing session against a certified calibration gas. The mean $\dot{V}O_2$ for the last 20 s at 40% PAP was 31 ± 5 ml kg^{-1} min^{-1} (mean ± SD). The corresponding value for the last 10 s at 110% PAP was 51 ± 6 ml kg^{-1} min^{-1}. Note that only at 40% PAP this $\dot{V}O_2$ measurement is at steady state, at 110% PAP, $\dot{V}O_2$ would be expected to continue to rise until $\dot{V}O_{2\,\mathrm{peak}}$ is reached and/or exhaustion.

2.5. Measurement of SO_2 and [Hb_{tot}] changes

Optical attenuation changes, ΔA_{λ_i}, were obtained with a NIRS monitor (NIRO-200, Hamamatsu Photonics KK, Japan) with a 6 Hz sampling frequency and three wavelengths ($\lambda_1 = 778$, $\lambda_2 = 812$ and $\lambda_3 = 850$ nm). The optical source and detector were positioned on the medial line of the shaved right *vastus lateralis*, one third of the distance from the lateral epicondyle to the greater trochanter of the femur. Only one detection channel was used with an interoptode distance of $L = 3.5$ cm.

The time derivatives of [HbO_2] and [Hb] (μM s^{-1}) were obtained from the optical attenuation changes by using the technique proposed by Hoshi *et al* (1997). This method reduces the unwanted influence of tissue scattering changes (Hoshi *et al* 1997) that may be significant during exercise (Ferreira *et al* 2007). Briefly, the measured attenuation can be described as

$$A_{\lambda_i} = A^0_{\lambda_i} + \Delta A_{\lambda_i} = \left\{\epsilon^{\mathrm{Hb}}_{\lambda_i}[\mathrm{Hb}] + \epsilon^{\mathrm{HbO_2}}_{\lambda_i}[\mathrm{HbO_2}]\right\} l + \mu^{\mathrm{bg}}_{a,\lambda_i} l + G_{\lambda_i}, \tag{1}$$

where A_{λ_i} is the attenuation at the wavelength λ_i ($i \in \{1, 2, 3\}$). The parameters $\epsilon^{\mathrm{HbO_2}}_{\lambda_i}$ and $\epsilon^{\mathrm{Hb}}_{\lambda_i}$ are the specific extinction coefficients for oxy- (HbO_2) and deoxy-haemoglobin (Hb). The parameter l is the differential path length. The parameter $\mu^{\mathrm{bg}}_{a,\lambda_i}$ is the absorption coefficient accounting for all background absorbers (e.g. myoglobin, fat) which are considered not to change significantly during the time and in particular during one pedal cycle. G_{λ_i} is a function which depends on scattering coefficients, scattering phase functions, geometry but not on absorption coefficients. The parameter l is defined as $l = \mathrm{DPF} \times L$; where DPF = 5 is the differential path length factor for the muscle (Cheatle *et al* 1991, Duncan *et al* 1995). The correction factors for the wavelength dependence of path length are embedded within the specific extinction coefficients (Essenpreis *et al* 1993). The parameter $A^0_{\lambda_i}$ is constant for a given wavelength which accounts for any time-invariant attenuation. By further following the procedure of Hoshi *et al* (1997), the time (t) derivative of the difference between two A_{λ_i}-couples is calculated, and an explicit expression for [Hb] and [HbO_2] in matrix notation is obtained as

$$\begin{pmatrix} [\dot{\mathrm{Hb}}] \\ [\dot{\mathrm{HbO_2}}] \end{pmatrix} = \frac{1}{lC} \begin{bmatrix} \left(\epsilon^{\mathrm{HbO_2}}_{850} - \epsilon^{\mathrm{HbO_2}}_{812}\right) & \left(\epsilon^{\mathrm{HbO_2}}_{812} - \epsilon^{\mathrm{HbO_2}}_{778}\right) \\ \left(\epsilon^{\mathrm{Hb}}_{812} - \epsilon^{\mathrm{Hb}}_{850}\right) & \left(\epsilon^{\mathrm{Hb}}_{778} - \epsilon^{\mathrm{Hb}}_{812}\right) \end{bmatrix} \begin{pmatrix} \Delta\dot{A}_{778} - \Delta\dot{A}_{812} \\ \Delta\dot{A}_{850} - \Delta\dot{A}_{812} \end{pmatrix}, \tag{2}$$

where the dot represents the time derivative. The 2 × 2 matrix contains the specific extinction coefficients where the suitable values for the index λ_i were substituted. The components of the 2 × 1 column vector on the right-hand side of equation (2) are expressed in terms of the time derivatives of the measured attenuation changes; the constant terms $A^0_{\lambda_i}$ have been eliminated

by the differentiation procedure. The constant C is the determinant of the matrix shown in equation (2). Intuitively, $[\dot{\mathrm{Hb}}]$ and $[\dot{\mathrm{HbO}}_2]$ describe the *net* flow of Hb and HbO_2 molecules entering (positive time derivative) or leaving (negative time derivative) the observed muscle ROI. The time derivatives of the ΔA_{λ_i} terms were obtained by applying a cubic B-spline model to ΔA_{λ_i} and then by taking the finite differences (Unser 1999).

The $[\mathrm{Hb_{tot}}]$ time derivative is defined as

$$[\dot{\mathrm{Hb}}_{\mathrm{tot}}] := [\dot{\mathrm{Hb}}] + [\dot{\mathrm{HbO}}_2]. \tag{3}$$

The *net* blood flow $[\dot{\mathrm{Hb}}_{\mathrm{tot}}]$ is non-zero only if there is an instantaneous net quantity of blood entering or leaving the observed ROI; a condition classically described as an increase/decrease in tissue 'blood volume'. To eliminate any ambiguity, we stress that the *net* blood flow $[\dot{\mathrm{Hb}}_{\mathrm{tot}}]$ is not the total tissue blood flow but only the $[\dot{\mathrm{Hb}}_{\mathrm{tot}}]$ flow of blood into the ROI accessed by the muscle pump. Our method is therefore not directly comparable to methods attempting to measure blood flow in the *entire* NIR interrogated region (see e.g. Ferreira *et al* (2005) or Bauer *et al* (2007)).

In this way, the instantaneous SO_2 of the instantaneous *net* blood flow $[\dot{\mathrm{Hb}}_{\mathrm{tot}}]$ can be written as

$$SO_2 = \frac{[\dot{\mathrm{HbO}}_2]}{[\dot{\mathrm{Hb}}] + [\dot{\mathrm{HbO}}_2]} \times 100, \tag{4}$$

where $[\dot{\mathrm{Hb}}]$ and $[\dot{\mathrm{HbO}}_2]$ are computed from the NIRS experimental data, ΔA_{λ_i} and equation (2). It should be noted that instantaneous SO_2 obtained from equation (4) is not the same as tissue SO_2 measured using conventional NIRS techniques.

By numerically integrating $[\dot{\mathrm{Hb}}]$ and $[\dot{\mathrm{HbO}}_2]$, one obtains $[\Delta\mathrm{Hb}]$ and $[\Delta\mathrm{HbO}_2]$. The symbol Δ reminds us that the integrating constants are not known and that they were arbitrarily chosen such that $[\Delta\mathrm{Hb}] = [\Delta\mathrm{HbO}_2] = 0$ at the beginning of the exercise ($t = 0$). Thus, only absolute changes in concentration (μM) can be experimentally monitored with the present NIRS technique. The observed instantaneous $[\mathrm{Hb_{tot}}]$ change is expressed as

$$[\Delta\mathrm{Hb}_{\mathrm{tot}}] := \int [\dot{\mathrm{Hb}}_{\mathrm{tot}}]\,\mathrm{d}t = [\Delta\mathrm{Hb}] + [\Delta\mathrm{HbO}_2]. \tag{5}$$

2.6. Measurement of $\dot{O}_{2\mathrm{m}}$

By exploiting the time-dependent parameters SO_2 (equation (4)) and $[\Delta\mathrm{Hb}_{\mathrm{tot}}]$ (equation (5)), it is possible to derive $\dot{O}_{2\mathrm{m}}$. Before describing the relationship in detail, the procedure is intuitively summarized in the following. During exercise on a cycle ergometer, $[\Delta\mathrm{Hb}]$, $[\Delta\mathrm{HbO}_2]$ and $[\Delta\mathrm{Hb}_{\mathrm{tot}}]$ periodically increase and decrease at each pedal cycle (see section 3). When the subject pushes on the pedal, the muscle is contracted, and thus the blood is squeezed out from the muscle (i.e. $[\Delta\mathrm{Hb}_{\mathrm{tot}}]$ decreases). During the relaxation phase the muscle is relaxed and the blood can refill the vascular bed again (i.e. $[\Delta\mathrm{Hb}_{\mathrm{tot}}]$ increases). Moreover, at steady state, the total change in $[\Delta\mathrm{Hb}_{\mathrm{tot}}]$ (i.e. maximum minus minimum value during one pedal cycle) is the same for the relaxation and contraction phase and is defined as $[\overline{\Delta\mathrm{Hb}_{\mathrm{tot}}}]$. The $[\Delta\mathrm{Hb}]$ and $[\Delta\mathrm{HbO}_2]$ periodicity along the pedal cycles gives also by definition a periodicity for instantaneous SO_2 (equation (4)). The key point permitting us to derive $\dot{O}_{2\mathrm{m}}$ is that the knowledge of SO_2 and $[\Delta\mathrm{Hb}_{\mathrm{tot}}]$, during one pedal cycle, allows us to derive the number of O_2 molecules entering the observed muscle ROI during relaxation and the number of O_2 molecules leaving the same ROI during contraction. The difference between the two values gives the O_2 utilized by the muscle, i.e. the O_2 that has been consumed due to its

involvement in the oxidative metabolism. Dividing the number of O_2 molecules utilized by the muscle during the corresponding time interval results in $\dot{O}_{2m}$.

We translate now the above procedure in more mathematical terms. The instantaneous SO_2 obtained during one pedal cycle allows us to compute the mean saturation, $\overline{SO}_2$, of the *net* blood that enters or leaves the muscle ROI, during the relaxation or the contraction phase. The two values are obtained by integrating SO_2, weighted by the instantaneous '*net* blood flow', $[\dot{\mathrm{Hb}}_{tot}]$, over the suitable time interval:

$$\overline{SO}_2 = \frac{\int_{t_1}^{t_2} SO_2[\dot{\mathrm{Hb}}_{tot}]\,dt}{\int_{t_1}^{t_2}[\dot{\mathrm{Hb}}_{tot}]\,dt}, \tag{6}$$

where t_1 and t_2 are the start- and end-time of the relaxation or contraction phase. The denominator is the normalization factor allowing us to express $\overline{SO}_2$ in percentage.

Finally, $\dot{O}_{2m}$ can be estimated by taking the difference between the quantity of oxygen accumulated during the relaxation phase and the quantity of oxygen leaving the muscle ROI during the contraction phase:

$$\dot{O}_{2m} = \frac{4}{10cT_{contract}}(\overline{SO}_{2\,relax} - \overline{SO}_{2\,contract})[\overline{\Delta \mathrm{Hb}_{tot}}], \tag{7}$$

where $\overline{SO}_{2\,relax}$ and $\overline{SO}_{2\,contract}$ are the corresponding $\overline{SO}_2$ of the blood that enters or leaves the ROI during the relaxation and contraction phase, respectively. The parameter $T_{contract}$ is the duration of the contraction phase. The number 4 in the numerator accounts for the haemoglobin-to-O_2 molar ratio; the factor of 10 expresses $\dot{O}_{2m}$ per 100 g of tissue; and $c = 1.13$ g ml^{-1} is the specific density of the skeletal muscle (Woodward and White 1982).

2.7. Filtering out incoherent physiological phenomena by group averaging

The procedure presented in the previous section does not account for the fact that NIRS signals are also affected by other physiological phenomena, uncorrelated with oxidative metabolism or with the periodic blood flow kinetics previously described. During dynamic exercise, the complex geometry of the microvascular tree (Popel and Johnson 2005) may modulate SO_2 levels by 'spurious' redistribution of oxygenated and deoxygenated blood between the muscle ROI and the surrounding tissues. In this case, a change of SO_2 may not only be related to oxidative metabolic activity. While these particular blood redistribution patterns display periodic behaviour synchronized with the pedal cycles for each subject (or the $[\Delta\mathrm{Hb}]$, $[\Delta\mathrm{HbO}_2]$ tracings that include the 'spurious' patterns would not be periodic as observed), they are different between subjects. To overcome this problem, the $[\Delta\mathrm{Hb}]$ and $[\Delta\mathrm{HbO}_2]$ time-dependent data of all subjects were averaged by taking the grand-mean before deriving $\dot{O}_{2m}$ (see section 3 for the exact procedure). The averaging procedure has the effect to filter out incoherent patterns and to amplify the major features that are common to the group; in this case, the $[\Delta\mathrm{Hb}]$ and $[\Delta\mathrm{HbO}_2]$ changes were induced by the oxidative metabolism.

In general, in the text errors are given as standard deviations (SD).

3. Results

In figure 1, the various plots show $[\Delta\mathrm{Hb}]$, $[\Delta\mathrm{HbO}_2]$ and $[\Delta\mathrm{Hb}_{tot}]$ as a function of time for one typical subject. The origin of the time axis coincides with the beginning of the exercise. As expected, $[\Delta\mathrm{Hb}]$ globally increases for increasing mechanical power and $[\Delta\mathrm{HbO}_2]$ shows the opposite behaviour. The zoomed versions (figures 1(b), (d) and (f)) of figures 1(a), (c) and (e) clearly show the oscillations induced by muscle relaxation/contraction phases during

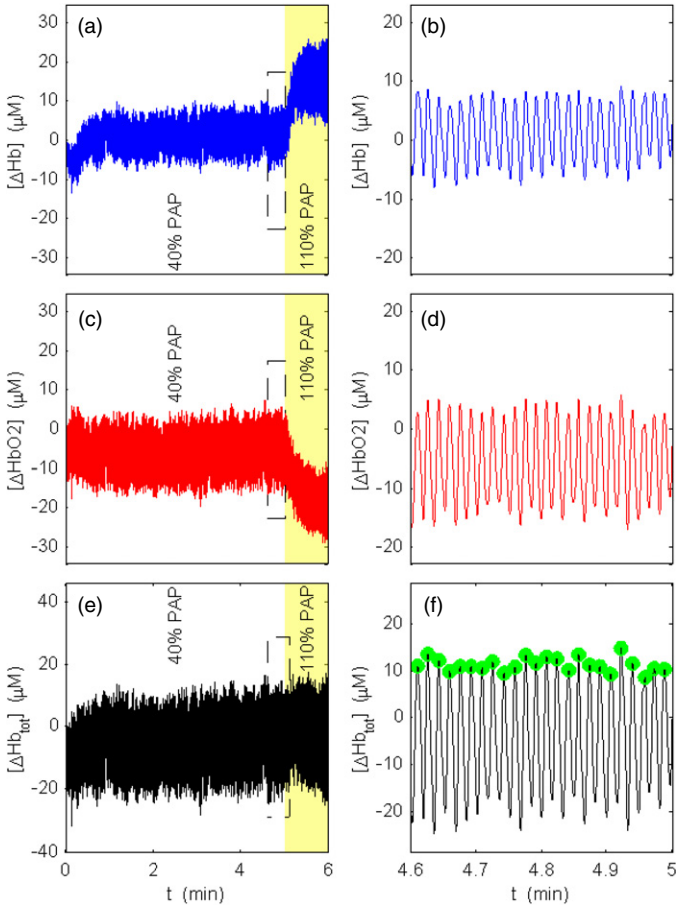

Figure 1. Deoxyhaemoglobin ([ΔHb]), oxyhaemoglobin ([ΔHbO_2]) and total haemoglobin ([ΔHb_{tot}]) concentration changes as a function of time (t) for one typical subject during exercise on a cycle ergometer. On panels (a), (c) and (e) the white and yellow background correspond to a work load of 40% of the peak aerobic power (PAP) and 110% PAP, respectively. At time 0 min the subject was at rest. Panels (b), (d) and (f) are the zoomed versions of the regions defined by the dashed squares on panels (a), (c) and (e), respectively. The green dots on panel (f) represent the maxima (see the text).

the pedalling cycles. A decreasing [ΔHb_{tot}] corresponds to the contraction phase (muscle is squeezed by pushing the pedal) and an increasing [ΔHb_{tot}] corresponds to the relaxation phase when the blood refills the vascular bed of the muscle ROI.

To investigate the behaviour of instantaneous SO_2 during one mean pedal cycle, the [ΔHb_{tot}] maxima were first automatically detected (figure 1(f), green points). Then, the different [ΔHb_{tot}] cycles were superimposed by taking the maxima as a time reference, and the grand-mean [ΔHb_{tot}] was computed (see schematic explanation in figure 2). This procedure is performed simultaneously for all the subjects and a given investigated work load, which leads to the group average. The mean duration of the chosen steady-state periods, at 40% PAP and 110% PAP were 112.0 ± 45.3 s and 25.5 ± 5.3 s, respectively. At 110% PAP, even if [ΔHb] and [ΔHbO_2] appear to be at 'steady state', the oxygen consumption might not be perfectly

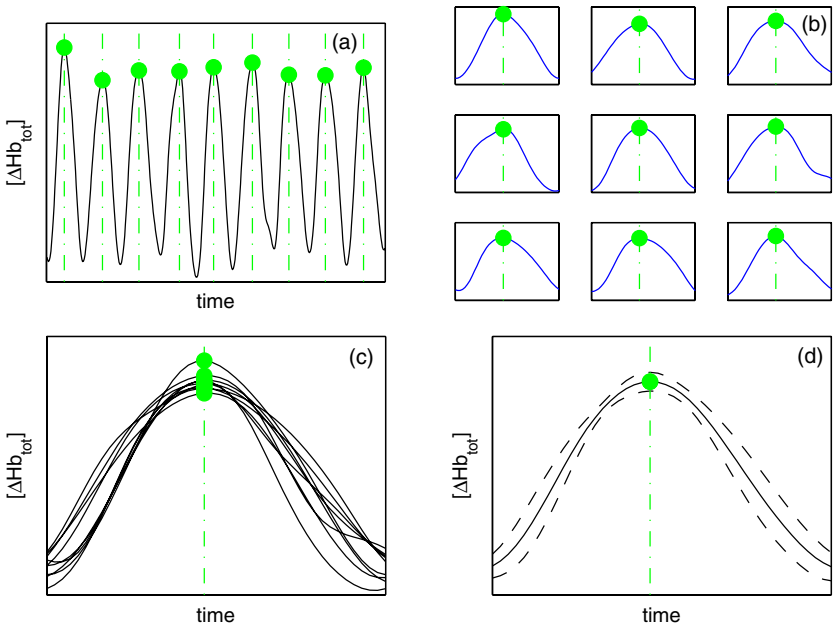

Figure 2. Schematic explaining how different $[\Delta Hb_{tot}]$ pedal cycles are decomposed to obtain an average pedal cycle. The green dots and dashed-dotted lines represent the position of the maxima. (a) Figure equivalent to figure 1(f) showing the $[\Delta Hb_{tot}]$ pedal cycles for a chosen stationary period, for a given subject; (b) each pedal cycle is separated from the others; (c) the different cycles are superimposed by synchronizing the maxima; (d) the grand-mean (continuous line) and the standard deviation (dashed lines) are computed using all the data from the 11 subjects.

constant. In this case, a short period minimizes the influence of any potential drift and has no consequences on the conclusions of the present paper. Due to the Shannon sampling theorem, the sampling frequency of 6 Hz allows us to observe $[\Delta Hb]$ and $[\Delta HbO_2]$ oscillations up to 3 Hz. Moreover, the above averaging procedure has the advantage of improving the features of a single 'mean' cycle; the spline interpolation procedure applied to obtain the time derivative guarantees the original values of $[\Delta Hb]$ and $[\Delta HbO_2]$ at the measurement time-points. Figure 3(a) and (b) show the resulting mean $[\Delta Hb_{tot}]$ as a function of time for 40% PAP and 110% PAP, respectively. The time duration of the two mean $[\Delta Hb_{tot}]$ cycles are obviously different due to the different pedal rates (60 and 80 rpm).

The corresponding mean $[\Delta \dot{H}b]$ and $[\Delta \dot{H}bO_2]$ kinetics were also derived and the results are reported in figures 3(e) and (f) for 40% PAP and 110% PAP, respectively. $[\Delta \dot{H}b] > 0$ (or $[\Delta \dot{H}bO_2] > 0$) means that deoxygenated (or oxygenated) blood is entering the muscle ROI with a subsequent increase in $[\Delta Hb]$ (or $[\Delta HbO_2]$). $[\Delta \dot{H}b] < 0$ (or $[\Delta \dot{H}bO_2] < 0$) represents an outflow and a decrease in $[\Delta Hb]$ (or $[\Delta HbO_2]$). Note that these changes represent *net* quantities, e.g. when a given HbO_2 flow enters the observed muscle ROI and simultaneously the same HbO_2 flow leaves the ROI, then the *net* flow, $[\Delta \dot{H}bO_2]$, is zero; however, this does not imply that there is no HbO_2 flow through the muscle.

By incorporating $[\Delta \dot{H}b]$ and $[\Delta \dot{H}bO_2]$ into equation (4) one obtains instantaneous SO_2. The computed SO_2 values are reported as a colour mapping in figures 3(a) and (b). This allows us to easily follow SO_2 during the corresponding $[\Delta Hb_{tot}]$ changes. To illustrate this further, instantaneous SO_2 is also reported in figures 3(c) and (d) for the 40% PAP and 110% PAP

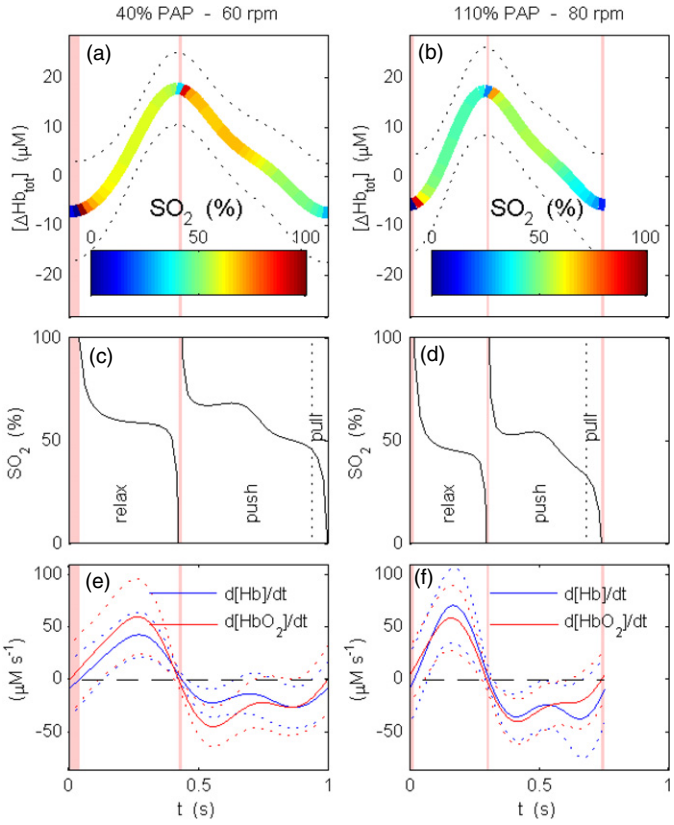

Figure 3. All the panels represent data on the group level. The pink regions represent the time intervals where muscle oxy- ($[\Delta\dot{\mathrm{H}}\mathrm{b}]$) and deoxy-haemoglobin ($[\Delta\dot{\mathrm{H}}\mathrm{bO}_2]$) have opposite sign. Panels (a), (c) and (e) report measurements acquired at 40% PAP and for a pedal rate of 60 revolutions per minute (rpm). Panels (b), (d) and (f) correspond to measurements acquired at 110% PAP and 80 rpm. Panels (a) and (b) show one mean $[\Delta\mathrm{Hb}_{\mathrm{tot}}]$ oscillation during one pedal cycle on a cycle ergomenter. The dotted lines represent the standard deviation. The colour map represents the instantaneous oxygen saturation values (SO_2) of the *net* blood flow entering/leaving the muscle (see the text). Panels (c) and (d) depict the colour-coded SO_2 values shown in panels (a) and (b). One pedal cycle includes three phases, i.e. relaxation, push and pull. Panels (e) and (f) show the group mean time derivative of the oxy- and deoxy-haemoglobin concentration changes during one pedal cycle, and the dotted lines are the standard deviations.

conditions, respectively. The pink vertical regions in figure 3 show the time periods where $[\Delta\dot{\mathrm{H}}\mathrm{b}]$ and $[\Delta\dot{\mathrm{H}}\mathrm{bO}_2]$ have opposite signs. Over these short time intervals it is not possible to compute SO_2 because the direction of the *net* flow is not well defined and these time intervals were neglected, which has almost no influence on $\dot{O}_{2\mathrm{m}}$ calculation. In fact, during the pink time intervals $[\Delta\dot{\mathrm{H}}\mathrm{b}_{\mathrm{tot}}] \approx 0$, and thus the contribution on $\overline{SO}_2$ (equation (6)) is negligible, and as a consequence the contribution on $\dot{O}_{2\mathrm{m}}$ (equation (7)) is also zero. For an explanation of the observed extreme values for SO_2, see subsection 4.2.

The $\overline{SO}_2$ values at 40% PAP were $\overline{SO}_{2\,\mathrm{relax}} = 61.28\%$ and $\overline{SO}_{2\,\mathrm{contract}} = 59.68\%$. At 110% PAP the values were $\overline{SO}_{2\,\mathrm{relax}} = 48.90\%$ and $\overline{SO}_{2\,\mathrm{contract}} = 46.95\%$. As expected, the $\overline{SO}_2$ values are lower at high work load, and $\overline{SO}_{2\,\mathrm{relax}} > \overline{SO}_{2\,\mathrm{contract}}$ for a given work load (i.e. some oxygen has been utilized by the muscle).

The concentration changes, $[\overline{\Delta Hb_{tot}}]$, for the filling (relaxation) and ejecting (contraction) phases during one mean pedal cycle were 25.14 μM and 22.86 μM at 40% PAP and 110% PAP, respectively. Considered that $[\Delta Hb_{tot}]$ is at steady state during this measurement, the filling and ejecting phases give the same $[\overline{\Delta Hb_{tot}}]$ value for a given percentage of PAP.

The duration, $T_{contract}$, of the ejecting phase ($[\Delta \dot{H}b_{tot}] < 0$) was 0.62 s and 0.48 s at 40% PAP and 110% PAP, respectively.

In this manner, by substituting $\overline{SO_{2\,relax}}$, $\overline{SO_{2\,contract}}$, $[\overline{\Delta Hb_{tot}}]$ and $T_{contract}$ in equation (7) one obtains for $\dot{O}_{2m}$, 13.78 μmol 100 g^{-1} min^{-1} and 19.72 μmol 100 g^{-1} min^{-1} for 40% PAP and 110% PAP, respectively. The $\dot{O}_{2m}$ values are expressed per 100 g of working muscle.

The mean heart rates were 124 ± 7 and 159 ± 5 at 40% PAP and 110% PAP, respectively.

4. Discussion and conclusions

4.1. Influence of myoglobin and adipose tissue

We have assessed the instantaneous SO_2 of the *net* blood flow entering or leaving an observed muscle ROI, during one mean pedal cycle (11 subjects), at steady state. The technique can be applied with any NIRS instrument that is fast enough to measure $[\Delta Hb]$ and $[\Delta HbO_2]$ oscillations induced by muscle contraction and relaxation.

The measured values are theoretically free from the influence of myoglobin because its concentration does not depend on blood volume pulsations. In other words, the time derivatives in equation (2) eliminate the myoglobin contribution by cancelling the terms $\mu_{a,\lambda_i}^{bg} l'$ in A_{λ_i} (equation (1)) for $i \in \{1, 2, 3\}$. This may be an important point, considering that some authors suggest that myoglobin concentration in muscle accounts for the largest part of the NIRS signal (Tran *et al* 1999, Marcinek *et al* 2007). This simplification obviously works only if the other chromophores (e.g. fat) implicitly included in μ_{a,λ_i}^{bg} are also constant over one pedal cycle, which is reasonably the case in the present situation.

Blood pulsations are generated by the contracting/relaxing muscle (Lutjemeier *et al* 2005); this physiological phenomenon does not exist in the adipose tissue layer (i.e. $[\Delta \dot{H}b] = [\Delta \dot{H}bO_2] \approx 0$ in this layer). For this reason, the computed SO_2 values (equation (4)) are also theoretically free from the influence of the blood contained in the adipose tissue layer and refers to the muscle only.

The previous paragraphs indirectly highlight the differences between classical NIRS-based tissue oxygen saturation measurements (McCully and Hamaoka 2000, Rolfe 2000, Boushel *et al* 2001, Quaresima *et al* 2003, Bhambhani 2004, Ferrari *et al* 2004, Hamaoka *et al* 2007, Wolf *et al* 2007), that include myoglobin and haemoglobin in adipose tissue, and the present SO_2 measurements.

4.2. Extreme values for SO_2

In figures 3(c) and (d) the relaxation and contraction phases reflect the same global SO_2 behaviour. It is interesting to notice the extreme instantaneous SO_2 values, i.e. SO_2 starts from 100% and then decreases to 0%. In practice, the oxygen saturation of the total blood flow entering the ROI cannot have a value higher than $\overline{SaO_2}$ (arterial blood) (see section 3), and thus certainly not 100%. However, as already mentioned, SO_2 refers to a *net* flow; this means that if $SO_2 = 100\%$, then the Hb inflow is perfectly compensated by a same Hb outflow, resulting in this manner in a zero *net* Hb flow and in a non-zero 'pure' *net* HbO_2 inflow (i.e. 100% saturated). A similar argument holds for 0% SO_2 and HbO_2.

4.3. $\overline{SaO_2}$ and $\overline{SO_{2\,\mathrm{relax}}}$

In pulse oximetry the arterial oxygen saturation $\overline{SaO_2}$ is calculated by measuring the pulsating arterial blood volume generated by the heart beats (Sinex 1999). In the present case the 'pulsations' are generated by the contracting/relaxing muscle. In section 3, it has been shown that $\overline{SO_{2\,\mathrm{relax}}}$ is 35.8% and 35.3% lower compared to $\overline{SaO_2}$ for 40% and 110% PAP, respectively. This result is not astonishing because the present technique simultaneously detects all the vessels going from the 'arterial' to the 'venous' side of the vascular tree that are filled during the relaxation phase and thus explains the smaller $\overline{SO_{2\,\mathrm{relax}}}$ values compared to $\overline{SaO_2}$. $\overline{SO_{2\,\mathrm{relax}}}$ gives new physiological information because it represents the local SO_2 of *net* inflowing blood into an exercising muscle. This should help us to better understand the mechanisms of oxygen transport in skeletal muscle during exercise. To our knowledge, $\overline{SO_{2\,\mathrm{relax}}}$ cannot be assessed by any other (even invasive) method. Obviously, other studies are necessary to better reveal the information contained in $\overline{SO_{2\,\mathrm{relax}}}$ and test its reliability; this will certainly be a subject for future experiments and mathematical simulations.

4.4. Push and pull

From figures 3(a) and (b) it appears that the duration of the filling ($[\Delta\dot{\mathrm{H}}\mathrm{b}_{\mathrm{tot}}] > 0$) and ejecting ($[\Delta\dot{\mathrm{H}}\mathrm{b}_{\mathrm{tot}}] < 0$) periods are not the same. In fact, high-level cyclists/triathletes naturally try to optimize the exercise efficiency not only by pushing but also by pulling on the pedals (Korff *et al* 2007). During the pulling phase the *vastus lateralis* is also contracted and this squeezes the muscle, generating even in this case a *net* blood outflow. This is the reason why, the contracting (push + pull; in figures 3(c) and (d)) phase last more than half pedal cycle. The pushing phase last by definition half the pedal cycle.

The total $[\Delta\mathrm{Hb}_{\mathrm{tot}}]$ change over one mean pedal cycle ($[\overline{\Delta\mathrm{Hb}_{\mathrm{tot}}}]$; see section 3) is smaller at 110% PAP than at 40% PAP, even if blood flow is in principle larger at a higher work load (Rådegran and Saltin, 1998). This is probably due to the fact that at 110% PAP, $[\overline{\Delta\mathrm{Hb}_{\mathrm{tot}}}]$ has less time to increase during the shorter relaxation phase (0.27 s versus 0.38 s at 40% PAP).

We noted that small periodic $[\Delta\mathrm{Hb}_{\mathrm{tot}}]$ pulsations are sometimes observed in the non-exercising muscle and in other tissues e.g. brain. Whilst in principle these signals can be used to measure oxygen consumption, it is important to note that this is only possible if oxygen is consumed between the rise and fall phases. For example a fully arterial fluctuation would not be productive to analyse.

4.5. $\dot{O}_{2\mathrm{m}}$ and $\dot{V}O_2$

As we have previously seen, the knowledge of $\overline{SO_{2\,\mathrm{relax}}}$, $\overline{SO_{2\,\mathrm{contract}}}$, $[\overline{\Delta\mathrm{Hb}_{\mathrm{tot}}}]$ and T_{contract} allows us to compute $\dot{O}_{2\mathrm{m}}$. Compared to other NIRS approaches for the assessment of oxygen consumption (Cheatle *et al* 1991, De Blasi *et al* 1993, Colier *et al* 1995, Sako *et al* 2001), the present one does not require the use of arterial occlusion, and in particular it is suitable to be applied to dynamic exercise at steady state.

The fundamental difference between $\dot{V}O_2$ and $\dot{O}_{2\mathrm{m}}$ is that while $\dot{O}_{2\mathrm{m}}$ refers to the working muscle only, $\dot{V}O_2$ also includes the contribution of the non-working muscles and all the other organs such as heart, lungs, bones, viscera, etc.

As reported above, the advantage of the present technique is that it is theoretically insensitive to the fat layer situated under the skin. In fact, it was previously demonstrated (Binzoni *et al* 1998) that a difference in adipose tissue thickness going from 0.35 cm to 1 cm produces a 75% underestimation of the actual resting $\dot{O}_{2\mathrm{m}}$ (measurements made with an interoptode distance of 3 cm) if the fat layer is not subtracted.

4.6. Future work

Considering the capability of the present technique to perform localized $\overline{SO}_{2\,\mathrm{relax}}$ and $\dot{O}_{2\mathrm{m}}$ measurements and the known spatial variability of muscle oxygenation (Niwayama *et al* 2000, Miura *et al* 2001, Quaresima *et al* 2001, Niwayama *et al* 2002, Quaresima *et al* 2004), it would be very interesting to investigate in the future if this variability also manifests itself for $\overline{SO}_{2\,\mathrm{relax}}$ or $\dot{O}_{2\mathrm{m}}$. Finally, we highlight the fact that NIRS is probably the unique approach allowing the investigation of the influence of local temperature changes on the oxidative metabolism of small muscle masses in humans (Binzoni *et al* 2002). The present work might open new possibilities in this domain.

In conclusion, we hope that this preliminary work will stimulate new ideas to further improve the proposed technique that represents, to our knowledge, the only non-invasive tool allowing localized (at the ROI level) $\overline{SO}_{2\,\mathrm{relax}}$ and $\dot{O}_{2\mathrm{m}}$ measurements in humans.

Acknowledgments

The authors would like to thank Hamamatsu Photonics KK and the EPRSC (EP/F006551/1 and EP/G005036/1) for their financial support of this work. This work was supported in part (DVDV) by the Swiss National Science Foundation (grant PP00P2-123438).

References

Bauer T A, Reusch J E, Levi M and Regensteiner J G 2007 Skeletal muscle deoxygenation after the onset of moderate exercise suggests slowed microvascular blood flow kinetics in type 2 diabetes *Diabetes Care* **30** 2880–5

Berne R M and Levy M 1998 *Physiology* (St Louis, MO: Mosby)

Bhambhani Y N 2004 Muscle oxygenation trends during dynamic exercise measured by near infrared spectroscopy *Can. J. Appl. Physiol.* **29** 504–23

Binzoni T, Ngo L, Hiltbrand E, Springett R and Delpy D 2002 Non-standard O(2) consumption–temperature curves during rest and isometric exercise in human skeletal muscle *Comp. Biochem. Physiol.* A **132** 27–32

Binzoni T, Quaresima V, Barattelli G, Hiltbrand E, Gürke L, Terrier F, Cerretelli P and Ferrari M 1998 Energy metabolism and interstitial fluid displacement in human gastrocnemius during short ischemic cycles *J. Appl. Physiol.* **85** 1244–51

Boushel R 2003 Metabolic control of muscle blood flow during exercise in humans *Can. J. Appl. Physiol.* **28** 754–73

Boushel R, Langberg H, Olesen J, Gonzales–Alonzo J, Blow J and Kjaer M 2001 Monitoring tissue oxygen availability with near infrared spectroscopy (NIRS) in health and disease *Scand. J. Med. Sci. Sports* **11** 213–22

Cheatle T R, Potter L A, Cope M, Delpy D T, Coleridge Smith P D and Scurr J H 1991 Near-infrared spectroscopy in peripheral vascular disease *Br. J. Surg.* **78** 405–8

Colier W N, Meeuwsen I B, Degens H and Oeseburg B 1995 Determination of oxygen consumption in muscle during exercise using near infrared spectroscopy *Acta Anaesthesiol. Scand. Suppl.* **107** 151–5

De Blasi R A, Cope M, Elwell C, Safoue F and Ferrari M 1993 Noninvasive measurement of human forearm oxygen consumption by near infrared spectroscopy *Eur. J. Appl. Physiol. Occup. Physiol.* **67** 20–5

Duncan A, Meek J H, Clemence M, Elwell C E, Tyszczuk L, Cope M and Delpy D T 1995 Optical pathlength measurements on adult head, calf and forearm and the head of the newborn infant using phase resolved optical spectroscopy *Phys. Med. Biol.* **40** 295–304

Ellsworth M L, Ellis C G, Goldman D, Stephenson A H, Dietrich H H and Sprague R S 2009 Erythrocytes: oxygen sensors and modulators of vascular tone *Physiology (Bethesda)* **24** 107–16

Essenpreis M, Elwell C E, Cope M, van der Zee P, Arridge S R and Delpy D T 1993 Spectral dependence of temporal point spread functions in human tissues *Appl. Opt.* **32** 418–25

Ferrari M, Mottola L and Quaresima V 2004 Principles, techniques, and limitations of near infrared spectroscopy *Can. J. Appl. Physiol.* **29** 463–87

Ferreira L F, Hueber D M and Barstow T J 2007 Effects of assuming constant optical scattering on measurements of muscle oxygenation by near-infrared spectroscopy during exercise *J. Appl. Physiol.* **102** 358–67

Ferreira L F, Townsend D K, Lutjemeier B J and Barstow T J 2005 Muscle capillary blood flow kinetics estimated from pulmonary O_2 uptake and near-infrared spectroscopy *J. Appl. Physiol.* **98** 1820–8

Haisch C 2009 Quantitative analysis in medicine using photoacoustic tomography *Anal. Bioanal. Chem.* **393** 473–9
Hamaoka T, McCully K K, Quaresima V, Yamamoto K and Chance B 2007 Near-infrared spectroscopy/imaging for monitoring muscle oxygenation and oxidative metabolism in healthy and diseased humans *J. Biomed. Opt.* **12** 062105
Hoshi Y, Hazeki O, Kakihana Y and Tamura M 1997 Redox behavior of cytochrome oxidase in the rat brain measured by near-infrared spectroscopy *J. Appl. Physiol.* **83** 1842–8
Korff T, Romer L M, Mayhew I and Martin J C 2007 Effect of pedaling technique on mechanical effectiveness and efficiency in cyclists *Med. Sci. Sports Exerc.* **39** 991–5
Leung T S, Wittekind A, Binzoni T, Beneke R, Cooper C E and Elwell C E 2010 Muscle oxygen saturation measured using 'cyclic NIR signals' during exercise *Adv. Exp. Med. Biol.* **662** 183–90
Lutjemeier B J, Ferreira L F, Poole D C, Townsend D and Barstow T J 2008 Muscle microvascular hemoglobin concentration and oxygenation within the contraction–relaxation cycle *Respir. Physiol. Neurobiol.* **160** 131–8
Lutjemeier B J, Miura A, Scheuermann B W, Koga S, Townsend D K and Barstow T J 2005 Muscle contraction-blood flow interactions during upright knee extension exercise in humans *J. Appl. Physiol.* **98** 1575–83
Marcinek D J, Amara C E, Matz K, Conley K E and Schenkman K A 2007 Wavelength shift analysis: a simple method to determine the contribution of hemoglobin and myoglobin to *in vivo* optical spectra *Appl. Spectrosc.* **61** 665–9
McCully K K and Hamaoka T 2000 Near-infrared spectroscopy: what can it tell us about oxygen saturation in skeletal muscle? *Exerc. Sport Sci. Rev.* **28** 123–7
Miura H, McCully K, Hong L, Nioka S and Chance B 2001 Regional difference of muscle oxygen saturation and blood volume during exercise determined by near infrared imaging device *Japan. J. Physiol.* **5** 599–606
Niwayama M, Kohata D, Shao J, Kudo N, Hamaoka T, Katsumura T and Yamamoto K 2000 Development of 200-channel mapping system for tissue oxygenation measured by near-infrared spectroscopy *Proc. SPIE* **4082** 48–56
Niwayama M, Yamamoto K, Kohata D, Hirai K, Kudo N, Hamaoka T, Kime R and Katsumura T 2002 A 200-channel imaging system of muscle oxygenation using CW near-infrared spectroscopy *IEICE Trans. Inf. Syst.* E **85-D** 115–23
Popel A S and Johnson P C 2005 Microcirculation and hemorheology *Annu. Rev. Fluid Mech.* **37** 43–69
Quaresima V, Colier W N, van der Sluijs M and Ferrari M 2001 Nonuniform quadriceps O_2 consumption revealed by near infrared multipoint measurements *Biochem. Biophys. Res. Commun.* **285** 1034–39
Quaresima V, Ferrari M, Franceschini M A, Hoimes M L and Fantini S 2004 Spatial distribution of vastus lateralis blood flow and oxyhemoglobin saturation measured at the end of isometric quadriceps contraction by multichannel near-infrared spectroscopy *J. Biomed. Opt.* **9** 413–20
Quaresima V, Lepanto R and Ferrari M 2003 The use of near infrared spectroscopy in sports medicine *J. Sports Med. Phys. Fitness* **43** 1–13
Rådegran G and Saltin B 1998 Muscle blood flow at onset of dynamic exercise in humans *Am. J. Physiol.* **274** H314–22
Rolfe P 2000 *In vivo* near-infrared spectroscopy *Annu. Rev. Biomed. Eng.* **2** 715–54
Sako T, Hamaoka T, Higuchi H, Kurosawa Y and Katsumura T 2001 Validity of NIR spectroscopy for quantitatively measuring muscle oxidative metabolic rate in exercise *J. Appl. Physiol.* **90** 338–44
Sinex J E 1999 Pulse oximetry: principles and limitations *Am. J. Emerg. Med.* **17** 59–67
Tran T K, Sailasuta N, Kreutzer U, Hurd R, Chung Y, Mole P, Kuno S and Jue T 1999 Comparative analysis of NMR and NIRS measurements of intracellular PO_2 in human skeletal muscle *Am. J. Physiol.* **276** R1682–90
Unser M 1999 Spline. A perfect fit for signal and image processing *IEEE Signal Process. Mag.* **16** 22–38
Wang L V 2008 Prospects of photoacoustic tomography *Med. Phys.* **35** 5758–67
Wang L V 2009 *Photoacoustic Imaging and Spectroscopy* (New York: CRC Press)
Wolf M, Ferrari M and Quaresima V 2007 Progress of near-infrared spectroscopy and topography for brain and muscle clinical applications *J. Biomed. Opt.* **12** 062104
Woodward H Q and White D R 1982 The composition of body tissues *Br. J. Radiol.* **59** 1029–219
Zhang E Z, Laufer J G, Pedley R B and Beard P C 2009 *In vivo* high-resolution 3D photoacoustic imaging of superficial vascular anatomy *Phys. Med. Biol.* **54** 1035–46